PROCEEDINGS OF SCIENCE

Investigating the Low-State of NGC 1275 with VERITAS and Multi-wavelength Observations

Anjana Kaushik Talluri[a,b,*] **for the VERITAS Collaboration**

[a] *School of Physics & Astronomy, 116 Church St SE, Minneapolis, USA*

[b] *Minnesota Institute for Astrophysics, 116 Church St SE, Minneapolis, USA*

E-mail: telid001@umn.edu

The VERITAS observatory is a ground-based imaging atmospheric Cherenkov telescope array that detects very-high-energy (VHE; E>100 GeV) gamma-ray emission from a range of astrophysical sources including more than ~89 Active Galactic Nuclei (AGN). At VHE, in contrast to the dominant blazar population, very few radio galaxies are detected. NGC 1275 (3C 84) is a radio galaxy in the nearby Perseus cluster (z~0.0176). Extensive VLBI observations of NGC 1275 reveal a complex morphology that has evolved with time. The origin of the VHE emission in both flaring and non-flaring states of NGC 1275 is still not entirely understood. In the current study, we present the low-state spectral energy distribution of NGC 1275 constructed with multi-wavelength observations from ALMA, ATLAS, *Swift*-UVOT, *Swift*-XRT, *Fermi*-LAT and VERITAS over the period 2012-2017. We find that the low-state emission is well explained by a single-zone Synchrotron self-Compton model which favors a large emission region.

High Energy Phenomena in Relativistic Outflows VIII (HEPROVIII)
23-26 October, 2023
Paris, France

[*] Speaker

PoS(HEPROVIII)079

1. Introduction

The dominant extragalactic sources at Very High Energies (VHE; E>100 GeV) are blazars, active galactic nuclei (AGN) with relativistic plasma jets oriented very near to our line-of-sight (LOS) [1]. In contrast, very few radio galaxies (RGs), AGN with misaligned jets to the LOS, are detected in VHE. Owing to their large jet-viewing angles, there is decreased Doppler boosting of the jet emission along the LOS and this results in a detection bias to nearby RGs. Despite extensive studies, the exact mechanism(s) of VHE gamma-ray emission in such sources remains unclear.

Due to the ease of detection in their high flux states, a substantial body of research is focused on bright flaring states of jetted AGN [2–4]. In contrast, jetted AGN in their low flux states require longer integration times to obtain enough photons for a detection. Consequently, the baseline state behavior of these sources remains relatively poorly understood. This is particularly true for the few RGs detected in VHE. Nevertheless, characterizing both low and high flux states is imperative to understand the underlying mechanisms governing VHE emission in jetted AGN, especially in the case of RGs.

1.1 Broadband SED

As with blazars, the broadband SED of RGs is typically characterized by two peaks: the lower frequency peak (IR to X-ray) corresponds to the synchrotron emission from electrons gyrating along the magnetic field in the jet, and the higher frequency peak (hard X-ray to γ-ray) is thought most likely to arise from inverse-Compton (IC) upscattering of different seed photon populations by the relativistic electrons in the jet. These can include the optical/UV synchrotron photons themselves (Synchrotron self-Compton or SSC), or photons from the surrounding regions in the AGN or from the ambient Cosmic Microwave Background (CMB) radiation (external inverse-Compton or EIC).

The TeV emission in many blazars in both the quiescent and flaring states is well explained by the leptonic SSC model [5–7] but is more challenging in the case of radio galaxies such as AP Librae [8] or Cen A [9], where the IC component is much broader than can be produced with a simple one-zone model. An alternative mechanism proposed that can successfully explain the HE-VHE emission in RGs with larger viewing angles ($\theta \sim 20°$) is the spine-layer configuration for the jet wherein a faster internal spine is surrounded by a slower-moving outer sheath layer [10, 11].

1.2 NGC 1275 (3C 84)

NGC 1275 (R.A.= $3^{h}\,19^{m}\,48^{s}$, decl.= $41°\,30'\,42''$; J2000.0), the central galaxy of the Perseus cluster, is well studied across various wavebands. Extensive VLBI observations provide evidence of a complex morphology that has evolved with time: around 2012 there was an initial brightening of C3 (a component associated with a radio outburst in 2005), followed by a breakout phase around the time of a gamma-ray flare in 2017, followed by C3 dimming significantly by 2020 [12].

Both MAGIC [Major Atmospheric Gamma Imaging Cherenkov; 13] and VERITAS [Very Energetic Radiation Imaging Telescope Array System; 14] telescopes have reported several significant detections of NGC 1275 in the VHE band in this time period [15–19].

A study by [20] looked at the broadband SED of NGC 1275 across 2009 to 2011 with multi-wavelength observations from *Swift*-XRT, *Fermi*-LAT, and MAGIC. Specifically, the study looked at two time periods, campaign I: October 2009-February 2010 and campaign II: August 2010-February 2011 and modeled the low-state emission in NGC 1275 with a single-zone SSC model.

In the current study, we focused on the low-state of NGC 1275 with long-term VHE observations from VERITAS over 2012-2017. We present the preliminary low-state multi-wavelength SED of NGC 1275 constructed with simultaneous observations from ALMA, ATLAS, *Swift*-UVOT, *Swift*-XRT, *Fermi*-LAT and VERITAS telescopes over the period 2012-2017 fitted to a single-zone SSC model. We find that the single-zone SSC model explains the low-state emission well.

2. Low State Selection

In order to build the low state multi-wavelength SED of NGC 1275, we first selected a low-state across all instruments over the time period of interest. The strategy employed in the selection of low-state data is outlined below:

1. Light curves were constructed for each waveband between 2012-2017.
2. A threshold was set to identify any flares within each band. Any potential high states identified with an additional threshold were also removed from each band.
3. Time constraints were applied to all datasets to ensure as much simultaneity between the bands as possible.
4. When a flare was identified in one band, simultaneous data were removed from the other bands as well.

3. Observations and Data Analysis

Below, we provide a summary of the observations and data analysis employed in each waveband.

3.1 VERITAS

NGC 1275 is regularly monitored by VERITAS; long-term observations over 2012-2017 were utilized to determine a low-state. The total low-state exposure is 53h, and analysis with two independent packages resulted in a 12σ significance of detection. The average low-state integral flux above 200 GeV was estimated to be around ~2.2% Crab. This estimate is in agreement with the MAGIC low-state flux reported in [20].

3.2 *Fermi*-LAT

Fermi-LAT observations in the range 0.1 GeV and 300 GeV over the time period of interest were obtained. We used the 4FGL *Fermi*-LAT source catalog [21] and obtained all point sources within a region of radius of 25° centered on NGC 1275 (4FGL J0319.8+4130). We utilized the open source python package `Fermipy v1.2` for the analysis [22].

As shown in [23], the low state inverse-Compton SED peak constructed with simultaneous *Fermi*-LAT and VERITAS data over 2012-2017 was found to fit best to a power-law with a sub-exponential cutoff model with a cutoff-energy of ~16 GeV. For further details on the *Fermi*-LAT and VERITAS analyses and the Compton SED fit, we refer the reader to [23].

3.3 *Swift*-XRT

A preliminary analysis of *Swift*-XRT observations over 2012-2017 was carried out with `XRTDAS` software package and `xspec` (v12.13) distributed under `HEASoft` (v6.31.1). Annular regions were used in source (in the PC mode) and background (in both PC and WT modes) spectra extraction to avoid pile-up. The data were fit to `phabs*powerlaw` to account for galactic nH absorption and source emission. We plan to re-model *Swift*-XRT data to also account for thermal emission from the hot cluster gas.

3.4 *Swift*-UVOT

The *Swift*-UVOT (Ultra-Violet and Optical Telescope) data were obtained over the period of interest in all the available filters using the online interactive UVOT analysis tool associated with the SED builder [1]. Fluxes were extracted from the image through aperture photometry; we utilized a circular source region of radius 5" and an annular background region with inner and outer radii of 20" and 30" respectively. The data were de-reddened and corrected for host galaxy emission. The error bar on the SED data was estimated to be the root-mean-square error (RMSE).

3.5 ATLAS

The Asteroid Terrestrial-impact Last Array System [ATLAS; 24] observations of NGC 1275 in the R filter over the time period of interest were analyzed and corrected for extinction and host galaxy emission. The SED flux data were weighted-averaged to obtain a single data point. The error on this data point was estimated as the RMSE.

3.6 ALMA

Multiple observations of NGC 1275 from the Atacama Large Millimeter/Sub-Millimeter Array (ALMA) in different radio frequencies were analyzed [25] with the Common Astronomy Software Applications (CASA) package. In the current study, we included the SED flux points from [25] that satisfied the aforementioned low-state selection criteria. We assumed a flux variation of 10% which is a typical estimate for the minimum flux variation of a source in the radio band. To derive more accurate error estimates, we will examine flux variation in the associated radio bands in an upcoming paper.

4. Multi-wavelength SED modeling

The low-state broadband SED was fitted to a single-zone SSC model with the latest version of `Bjet-MCMC` tool [26]. The underlying leptonic particle distribution was assumed to be a broken power-law. We fitted the SED to a single-zone SSC emission model with an upper constraint on the jet viewing angle at 18° to accommodate VHE emission. The hyperparameters of the MCMC fit include the number of iterations of the walkers (steps), the number of walkers exploring the parameter space simultaneously (walkers) and the initial set of iterations in which the algorithm explores the parameter space and moves towards regions of higher probability (burn-in). These hyperparameters were tuned to the following values: 6500 steps, 200 walkers and a burn-in of 250. The best fitting SED is shown in Fig. 1 and the corresponding model parameters are displayed in Table 1.

5. Conclusion

We presented the preliminary low-state multi-wavelength SED of NGC 1275 over 2012-2017 fit to a single-zone SSC model. The model predicts a large emission zone (~parsec scale) responsible for the low-state multi-wavelength emission of NGC 1275. Such a large emission region may not be accommodated by emission from the core. This may be suggestive of the radio-zone C3 as a potential TeV emitter in the low state, which is consistent with SED modeling of the 2017 NGC 1275 flare in [25]. A detailed interpretation and discussion of these results along with the multi-wavelength lightcurves will be presented in an upcoming paper.

[1]https://tools.ssdc.asi.it/SED/

PoS(HEPROVIII)079

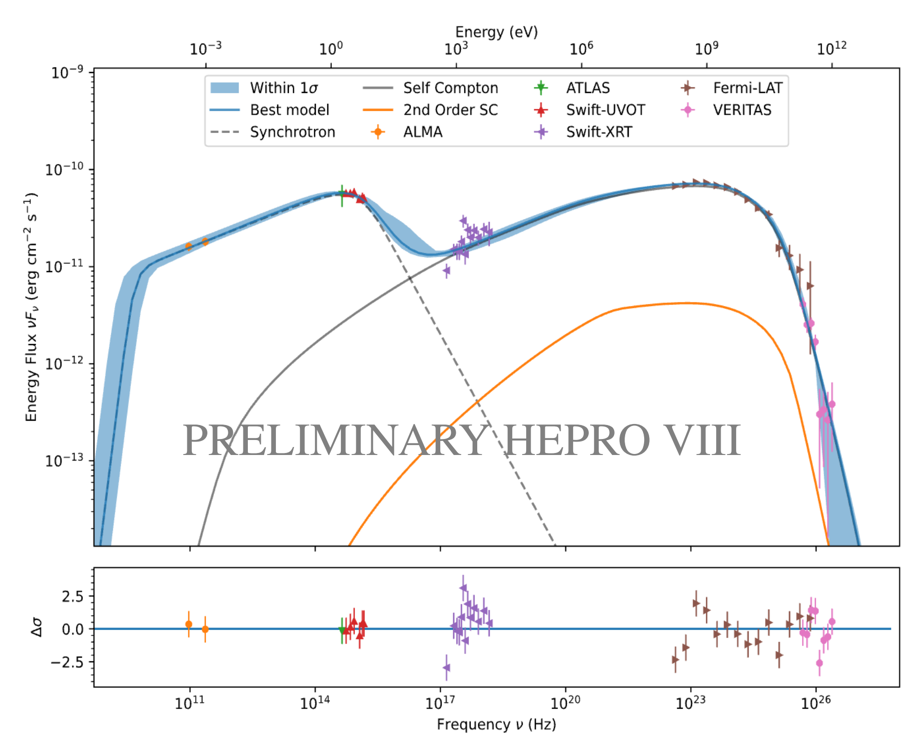

Figure 1: Low-state MWL SED with data from 2012-2017 fitted to a single-zone SSC model. The best fit and the 1sigma errors are shown in blue. The synchrotron bump is indicated by a dotted line and the inverse-Compton bump in a solid black line. The second order SSC component is shown in orange.

Parameter	**Best Value with 1σ error**
δ	$2.48^{+0.22}_{-1.42}$
K [cm^{-3}]	$7.4^{+12.3}_{-6.3} \times 10^3$
α_1	$2.7^{+0.04}_{-0.05}$
α_2	$4.6^{+0.4}_{-1}$
$\gamma_{\rm min}$	$6.5^{+28.5}_{-5.5} \times 10^1$
$\gamma_{\rm max}$	$576^{+424}_{-571} \times 10^6$
$\gamma_{\rm break}$	$1.04^{+0.95}_{-0.38} \times 10^4$
B [G]	$7.59^{+8.81}_{-4.12} \times 10^{-3}$
R [cm]	$2.3^{+7.7}_{-1.3} \times 10^{18}$
χ^2/dof	66.93 / 35 = 1.83

Table 1: Best fitting parameters of the single-zone SSC model with the corresponding 1σ errors. The parameters listed are the Doppler factor, particle density factor, first and second indices of the assumed broken powerlaw leptonic distribution, Lorentz factors of the radiating particles at the minimum, break, maximum of their distribution, magnetic field strength and blob radius. For additional information, we refer the reader to [26].

Acknowledgements

This research was partially supported by the National Science Foundation under grants PHY 2110737 and DGE-1922512. This research is supported by grants from the U.S. Department of

Energy Office of Science, the U.S. National Science Foundation and the Smithsonian Institution, by NSERC in Canada, and by the Helmholtz Association in Germany. This research used resources provided by the Open Science Grid, which is supported by the National Science Foundation and the U.S. Department of Energy's Office of Science, and resources of the National Energy Research Scientific Computing Center (NERSC), a U.S. Department of Energy Office of Science User Facility operated under Contract No. DE-AC02-05CH11231. We acknowledge the excellent work of the technical support staff at the Fred Lawrence Whipple Observatory and at the collaborating institutions in the construction and operation of the instrument.

References

[1] Rieger, F.M. *Gamma-Ray Astrophysics in the Time Domain*, *Galaxies* **7** (2019) 28

[2] Aharonian, F., Akhperjanian, A. G., Bazer-Bachi, A. R., et al. *An Exceptional Very High Energy Gamma-Ray Flare of PKS 2155-304*, *ApJ* **664** (2007) L71

[3] A. U. Abeysekara et al, *Gamma-Rays from The Quasar PKS 1441+25: Story of an Escape*, *ApJ* **815** (2015) L22

[4] Abeysekara, A. U., Benbow, W., Bird, R., et al. *The Great Markarian 421 Flare of 2010 February: Multiwavelength Variability and Correlation Studies*, *ApJ* **890** (2020) 97

[5] Maraschi, L., Ghisellini, G. & Celotti, A., *A Jet Model for the Gamma-Ray–emitting Blazar 3C 279*, *ApJL* **397** (1992) L5

[6] Bloom, S. D. & Marscher, A. P., *An Analysis of the Synchrotron Self-Compton Model for the Multi-Wave Band Spectra of Blazars*, *ApJ* **461** (1996) 657

[7] H. E. S. S. Collaboration, Abramowski, A., Acero, F., et al., *Discovery of TeV γ-ray emission from PKS 0447-439 and derivation of an upper limit on its redshift*, *A&A* **552** (2013) A118

[8] Roychowdhury, A., Meyer, E.T., Georganopoulos, M., et al., *Circumnuclear Dust in AP Librae and the Source of Its VHE Emission*, *ApJ* **924** (2022) 57

[9] M. Petropoulou, E. Lefa, S. Dimitrakoudis, & A. Mastichiadis, *One-zone synchrotron self-Compton model for the core emission of Centaurus A revisited*, *A&A* **562** (2014) A12

[10] Tavecchio F., Ghisellini G., *On the spine-layer scenario for the very high-energy emission of NGC 1275*, *MNRAS* **443** (2014) 1224-1230

[11] Ghisellini G. et al., *Structured jets in TeV BL Lac objects and radiogalaxies*, *A&A* **432** (2005) 401-410

[12] Motoki Kino et al., *Morphological Transition of the Compact Radio Lobe in 3C 84 via the Strong Jet–Cloud Collision*, *ApJL* **920** (2021) L24

[13] Aleksić J., Alvarez E. A., Antonelli L. A., et al., *Performance of the MAGIC stereo system obtained with Crab Nebula data*, *Aph* **35** (2012) 435-448

[14] Holder J., Atkins R. W., Badran H. M., et al., *The first VERITAS telescope*, *Aph* **25** (2006) 391

[15] Aleksic, J., Alvarez, E. A., Antonelli, L. A., et al., *Detection of very-high energy -ray emission from NGC 1275 by the MAGIC telescopes*, *A&A* **539** (2012) L2

[16] Benbow W., & the VERITAS Collaboration, *Highlights from the VERITAS AGN Observation Program* in 34th International Cosmic Ray Conference (ICRC) 2015 p. 821

[17] Mukherjee R., & VERITAS Collaboration, *VERITAS detection of the radio galaxy NGC 1275 with elevated very-high-energy gamma-ray emission*, The Astronomer's Telegram 2016, 9690 p1

[18] Mirzoyan R., *MAGIC detection of an increased activity from NGC 1275 at very-high-energy gamma rays*, The Astronomer's Telegram 2016, 9689 p1

[19] Mukherjee, R., & VERITAS Collaboration *VERITAS detection of the radio galaxy NGC 1275 with elevated very-high-energy gamma-ray emission*, The Astronomer's Telegram 2017, 9931, p1

[20] Aleksić J., et al., *Contemporaneous observations of the radio galaxy NGC 1275 from radio to very high energy γ-rays A&A* **564** (2014) A5

[21] Abdollahi, S., Acero, F., Ackermann, M., et al., *Fermi Large Area Telescope Fourth Source Catalog*, *ApJS* **247** (2020) 33

[22] Wood, M., Caputo, R., Charles, E., et al., *Fermipy: An open-source Python package for analysis of Fermi-LAT Data*, in 35th ICRC 2017 p. 824

[23] Talluri A. K., & VERITAS Collaboration, *Investigating the Quiescent State of NGC 1275 with VERITAS and Multi-wavelength Observations* in 38th ICRC 2023 p. 661

[24] Tonry, J. L., Denneau, L., Heinze, A. N., et al., *ATLAS: A High-cadence All-sky Survey System PASP* **130** (2018) 064505

[25] Rulten et al., *VERITAS observations of the radio galaxy NGC 1275*, in prep.

[26] Hervet, O., Johnson, C. A., & Youngquist, A., *BjetMCMC: A new tool to automatically fit the broadband SEDs of blazars*, *arXiv* **962** (2023) 140